

Chapter 4

Influence of Specific Interactions of Polyhedral Oligomeric Silsesquioxanes-Containing Poly(methyl methacrylate)/Phenolic Blends

Abstract

In this study, the homopolymers of the methyl methacrylate have been prepared using atom transfer radical polymerization (ATRP) techniques from the polyhedral oligomeric silsesquioxanes (POSS) initiator. These organic-inorganic hybrids contain under 10 wt% of POSS. The characterized data of POSS-poly(methyl methacrylate) (POSS-PMMA) are reported from analyses by gel permeation chromatography (GPC) and ^1H NMR spectroscopy. The miscibility behaviour and interactions in blends of POSS-PMMA with phenolic resins were observed. Experimental results showed that the glass transition temperatures (T_g) of the POSS-PMMA/phenolic blends by differential scanning calorimetry (DSC) were higher than that of the PMMA/phenolic blends. The positive q value of POSS-PMMA/phenolic blends decreases with the increase of molecular weight of POSS-PMMA. The negative q value of PMMA/phenolic blends also decreases with the increase of molecular weight of PMMA. This large positive deviation reveals that a strong inter-association interaction must exist between POSS-PMMA and phenolic resins. Fourier transform infrared (FT-IR) spectroscopy and two-dimensional infrared (2D IR) correlation spectroscopy show that inter-association hydrogen bonding interaction between PMMA and phenolic resins in POSS-PMMA/phenolic blends was smaller than that in PMMA/phenolic blends.

4.1 Introduction

Over the last several years, the interest in nanocomposites, which is the hybridization of inorganic materials and organic polymers on a molecular scale, has increased dramatically with the rapid growth of nanoscale technologies [1]. By adding inorganic materials into organic polymers, mechanical, thermal, electrical, and magnetic properties are changed from those of pure organic polymers. Nanocomposites, combining the important properties from inorganic materials and organic polymers, can create new unique properties such as high gas barrier [2], solvent resistance [3], UV light resistance, flame resistance property, and so on. These exceptional properties have received great attention in nanocomposites preparation and analysis with the promise of new applications in many fields, including optics, electricity, mechanics, and biochemistry.

In the research course of nanocomposites, the first method is that the inorganic-organic polymer hybrids could be prepared by the sol-gel reaction. The sol-gel reaction comprises the hydrolysis of Si-OR groups to Si-OH (silanol) groups and the condensation of the silanol groups into -Si-O-Si- linkages [4]. A three-dimensional silica gel network is constructed as the sol-gel reaction proceeds. One of the most attractive features of this method is its low processing temperature, which allows organic polymer to be incorporated into the silica matrix without decomposition. The second one is utilizing blends of polymers and montmorillonites (clays). This has been studied extensively because a small amount of well-dispersed clay layers in the polymer matrix can improve its mechanical and thermal properties. The inorganic layered silicate structure of the clay, however, does not permit it to disperse well in the organic polymer matrix and it is essential to pretreat the clay with appropriate surfactants [7]. The third one is utilizing the polyhedral oligomeric silsesquioxane (POSS). Polyhedral oligomeric silsesquioxanes (POSS) are one type of material capable of forming nanocomposites. The POSS moiety has a unique and well-defined structure that can be used for preparing hybrid materials with well defined structures. The properties of POSS

are unique since one or more of the organic groups can be made reactive for polymerization, while the remaining unreactive groups solubilize the inorganic core and allow for control over the interfacial interactions occurring between POSS and the polymer matrix. POSS units can be added to virtually all polymer types either by blending, grafting, or copolymerization reactions [6]. By incorporating the rigid Si-O cage into polymers, property enhancements such as increased thermal stability, reduced flammability, reduced viscosity, and lowered density have been observed. These property enhancements make POSS compounds of great interest to further improve high performance polymers and to develop multifunctional materials [7].

Poly(methyl methacrylate) (PMMA)/phenolic blends are well-known example of miscible polymer blends. The nature of intermolecular interactions in PMMA/phenolic blends has been extensively studied. The miscibility of polymer blends is commonly ascertained through the measurements of glass transition temperatures (T_g) by differential scanning calorimetry (DSC). The existence of a single composition- dependent T_g indicates miscibility on a scale of about 20-40 nm. As a rule, nuclear magnetic resonance (NMR) spectroscopy and resolution solid-state ^{13}C nuclear magnetic resonance (NMR) spectroscopy have been used to study the miscibility of polymer blends. Fourier transform infrared (FT-IR) spectroscopy, two-dimensional infrared (2D IR) correlation spectroscopy and X-ray photoelectron spectroscopy (XPS) have been also used to study interactions in polymer blends. For instance, Zhou et al. [8] carried out an XPS study on poly(styrene) (PS)/poly(2,6-dimethyl-1,4-phenylene oxide) (PPO) and found that methyl substitution of PS markedly reduces intermolecular interactions by existence of π -complexation between PS and PPO. On the basis of a solution NMR study on low molecular weight model compounds, Djordjevic and Porter [9] concluded that the main interaction was between the electrodeficient methyl groups of PPO and the π -orbitals of PS. We have recently reported an FT-IR study on star PMMA/phenolic blends and linear PMMA/ phenolic blends [10].

Atom transfer radical polymerization (ATRP) is one of living/controlled radical polymerization methods. ATRP has been shown to be a versatile technique for the controlled polymerization of many monomer classes, including acrylates [11], methacrylates [12], and styrenics [13] since 1995. Moreover, ATRP can yield polymers with low polydispersity and controlled molecular weight. Generally, ATRP syntheses are carried out at high temperatures either in the bulk or in nonaqueous media.

In this article, we report the preparation of the inorganic-organic polymer hybrids involving POSS compounds by ATRP. The ATRP conditions with copper (I) bromide/*N,N,N',N'',N'''*-pentamethyldiethylenetriamine (CuBr/PMDETA) as the catalyst system were employed for the polymerization of methyl methacrylate to generate well-defined homopolymers. Then, POSS-PMMA and PMMA were blended with phenolic resin, respectively. It is of interest to see whether hydrogen bonding interactions are changed in PMMA/phenolic and POSS-PMMA/phenolic blends. The characterized data are observed by gel permeation chromatography (GPC), ¹H NMR spectroscopy, differential scanning calorimetry (DSC), Fourier transform infrared (FT-IR) spectroscopy and two-dimensional infrared (2D IR) correlation spectroscopy.

4.2 Experimental Section

4.2.1 Materials

Isobutyltrisilanol-POSS was obtained from Hybrid Plastics Co. and used as received. Methyl methacrylate (MMA) was distilled from calcium hydride and stored under N₂. Copper (I) bromide (CuBr) was purified by washing with glacial acetic acid overnight, followed by absolute ethanol and ethyl ether, and then dried under vacuum. Amberlite IR-120 (H form) cation exchange resin, anisole, *N,N,N',N'',N''*-pentamethyldiethylenetriamine (PMDETA), methyl 2-bromopropionate (MBrP), triethylamine (TEA) and trichloro[4-(chloromethyl)phenyl]silane were all used as received. All solvents were distilled prior to use.

4.2.2 Characterization

Nuclear magnetic resonance spectroscopy (NMR). ¹H NMR spectra were recorded as solutions on a Bruker AM500 (500MHz) spectrometer, with the solvent proton signal as a standard.

Gel permeation chromatography (GPC). Molecular weights and molecular weight distributions were determined by GPC. GPC was conducted on a Waters 510 HPLC–equipped with a 410 Differential Refractometer, a UV detector, and three Ultrastyrigel columns (100, 500, and 10³ Å) connected in series in order of increasing pore size—using THF as an eluent at a flow rate of 0.6 mL/min. The molecular weight calibration curve was obtained using polystyrene standards.

Differential scanning calorimetry (DSC). Glass transition temperatures (*T_g*) were measured by DSC from Du-Pont (model 910 DSC-9000 controller). Heating rates were 20 °C/min, and a temperature range of 30-170 °C in nitrogen atmosphere. Approximately 4-6 mg sample was weighed and sealed in an aluminum pan. The sample was quickly cooled to 0 °C from the first scan and then scanned between 0 and 200 °C at a scan rate of 20 °C /min. The *T_g* was taken as the midpoint of the heat capacity transition between the upper and lower points of deviation from the extrapolated glass and liquid lines.

Fourier transform infrared spectroscopy (FT-IR). FT-IR spectra were obtained on a Nicolet Avatar 320 FT-IR Spectrometer, 32 scans at a resolution of 1 cm^{-1} were collected with a KBr disk at room temperature. The THF solution containing the sample was cast onto a KBr disk and dried under containing similar to that used in bulk preparation. The sample chamber was purged with nitrogen in order to maintain the film dryness.

Two-dimensional infrared correlation spectroscopy (2D IR). 2D IR correlation analysis was conducted using “Vector 3D” software (from Bruker Instrument Co.). All of the spectra were normalized before being subjected to the 2D correlation analyses. Shaded regions indicate the negative intensity of autopeaks or crosspeaks in 2D-correlation spectrum; unshaded regions indicate positive.

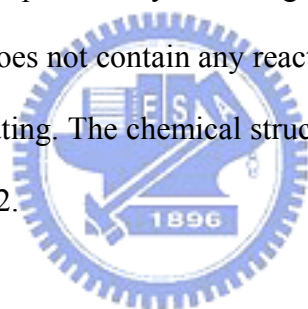
4.2.3 Synthesis of Initiator

The initiator, POSS-Cl, was prepared by reacting trichloro[4-(chloromethyl)phenyl] silane (1.00 mL, 5.61×10^{-3} mol) with isopropyltrisilanol-POSS (4.05 g, 5.11×10^{-3} mol) in the presence of triethylamine (2.20 mL, 1.54×10^{-2} mol) in 30.0 mL of dry THF under argon. The reaction flask was stirred at room temperature for 7.5 h, followed by filtration to remove the HNEt₃Cl byproduct. The clear THF solution was dropped into a beaker of acetonitrile and rapidly stirred. The resulting product was collected by filtration and dried in a vacuum. (4.61 g, 80 %). ¹H NMR (CDCl₃), δ : 7.59 (d, 2H), 7.33 (d, 2H), 4.52 (s, 2H), 1.92-1.62 (m, 7H), 1.09-0.85 (m, 42H), 0.75-0.48 (m, 14H) (Figure 4.1 (a)). The synthetic route for POSS-Cl is shown in Scheme 4.1.

4.2.4 Syntheses of Polymer

The typical ATRP protocol was as follows (Scheme 4.1). To prepare the POSS-PMMA polymers, the ATRP with CuBr/*N,N,N',N'',N''*-pentamethyldiethylenetriamine (PMDETA) was carried out. These molecular weights of POSS-PMMA ($M_n = 10,350\text{ g mol}^{-1}$ and $M_n = 29,700\text{ g mol}^{-1}$) were determined by GPC. In accordance with the controlled polymerization characteristics of ATRP, the polydispersity of the POSS-PMMA ($M_n = 10,350\text{ g mol}^{-1}$) is low

(PDI =1.15) and that of the POSS-PMMA ($M_n = 29,700 \text{ g mol}^{-1}$) is low (PDI =1.18). The linear PMMA polymers were also prepared by ATRP with methyl DL-2-bromopropionate monofunctional initiator. These molecular weights of PMMA ($M_n = 9,800 \text{ g mol}^{-1}$ and $M_n = 28,900 \text{ g mol}^{-1}$) were also determined by GPC. The polydispersity of the PMMA ($M_n = 9,800 \text{ g mol}^{-1}$) is low (PDI =1.15) and that of the PMMA ($M_n = 28,900 \text{ g mol}^{-1}$) is low (PDI =1.17). The ^1H NMR spectrums of POSS-PMMA and PMMA were shown in Figure 4.1 (b) and 4.1 (c). The phenolic resins was synthesized with sulfuric acid via a condensation reaction and with average molecular weights of $M_n = 500 \text{ g mol}^{-1}$ and $M_w = 1200 \text{ g mol}^{-1}$ that was described in the previous study. The chemical structure of the Novolac-type phenolic resin consists of phenolic rings bridge-linked randomly by methylene groups with 19% ortho–ortho, 57% ortho–para, and 24% para–para methylene bridges, identified by the solution ^{13}C NMR spectrum. The phenolic resin does not contain any reactive methylene group, which is capable of causing cross-linking on heating. The chemical structures of PMMA and phenolic resin are shown as follows in Scheme 4.2.



4.2.5 Blend Preparation

Desired composition containing POSS-PMMA or linear PMMA and phenolic resin was dissolved in THF at a concentration of 5 wt% and stirred for 6–8 h. The solution was allowed to evaporate slowly at $25 \text{ }^\circ\text{C}$ for 1 day on a Teflon plate and dried at $90 \text{ }^\circ\text{C}$ for 3 days to ensure total elimination of the solvent.

4.3 Results and Discussion

4.3.1 DSC Analyses

The most widely used criterion for the judgment of the miscibility behaviour of polymer blends is the existence of a single glass transition temperature (T_g). The T_g of PMMA ($M_n = 9,700 \text{ g mol}^{-1}$) (LPMMA) or POSS-PMMA ($M_n = 10,350 \text{ g mol}^{-1}$) (POSS-LPMMA)/phenolic blends dependence on composition is shown in Figure 4.2 (a) and 4.2 (b). The T_g of PMMA ($M_n = 28,900 \text{ g mol}^{-1}$) (HPMMA) or POSS-PMMA ($M_n = 29,700 \text{ g mol}^{-1}$) (POSS-HPMMA)/phenolic blends dependence on composition is shown in Figure 4.2 (c) and 4.2 (d). Each blend showed a composition-dependent T_g , showing that these are fully miscible blends with a homogeneous amorphous phase. A single T_g of POSS-PMMA/phenolic blends is higher than that of either individual polymer was observed. However, a single T_g of PMMA/phenolic blends is lower than that of either individual polymer was indicated. This large positive deviation reveals that a strong inter-association interaction must exist between POSS-PMMA and phenolic resins. It has been generally suggested that the T_g relationship to the composition of the miscible polymer blends follows the Kwei equation:

$$T_g = \frac{W_1 T_{g1} + kW_2 T_{g2}}{W_1 + kW_2} + qW_1 W_2 \quad (1)$$

where w_1 and w_2 are weight fractions of the components, T_{g1} and T_{g2} represent the corresponding glass transition temperatures, and k and q are fitting constants. In this study, $k = 1$ and $q = 35$ of POSS-LPMMA/phenolic blends, $k = 1$ and $q = -38$ of LPMMA/phenolic blends, $k = 1$ and $q = 23$ of POSS-HPMMA/phenolic blends and $k = 1$ and $q = -36$ of HPMMA/phenolic blends were obtained from the non-linear least-squares ‘best fit’ values (Figure 4.3 and 4.4). Here q is a parameter corresponding to the strength of hydrogen bonding in the blends, reflecting a balance between the breaking of the self-association and the forming of the inter-association hydrogen bonding. These positive q values of 23 (POSS-HPMMA) and 35 (POSS-LPMMA) were obtained, indicating a strong inter-association interaction between

POSS-PMMA and phenolic resins. Further, the incorporation of POSS into PMMA affects the interaction between PMMA and phenolic resins, especially at POSS-LPMMA. These q values of PMMA/phenolic blends were -36 (HPMMA) and -38 (LPMMA), indicating that a self-association interaction between PMMA and phenolic resins is stronger than an inter-association interaction. These q values show that the interactions in LPMMA/phenolic blends are similar to that in HPMMA/phenolic blends.

4.3.3 FT-IR Analyses

Chemical structures of PMMA and phenolic resins are shown in Scheme 4.1, containing IR carbonyl vibrations from the free and hydrogen-bonded of PMMA with phenolic resins. The phenolic unit may exist as free state, self-associated dimer, or inter-association with PMMA. Hence, states of PMMA and phenolic associations in these blends can be analyzed by FT-IR spectra. Figure 4.5 shows the scale-expanded infrared spectra in the hydroxyl-stretching region with various compositions of POSS-PMMA/phenolic and PMMA/phenolic blends at room temperature. The spectra of the pure phenolic resins shows a broad band at 3350 cm^{-1} and a shoulder at 3525 cm^{-1} , corresponding to the multimer hydrogen-bonded hydroxyl groups and the free hydroxyl groups, respectively. The intensity of the free hydroxyl bands both decreases with the increase of the POSS-PMMA or PMMA content in these blends. It is expected that large portion of these 'free' OH groups is consumed by forming the inter-association hydrogen bonds between the PMMA and the phenolic resins. Meanwhile, the band (at about 3435 cm^{-1}) appears with the increase of the PMMA content as the result of the decrease in the free hydroxyl band. In addition, portion of the self-association hydrogen bonds (at 3350 cm^{-1}) are broken off to form the inter-association hydrogen bonds [14]. This phenomenon depicts that a new distribution of hydrogen bonding formation resulting from the competition between hydroxyl–hydroxyl and hydroxyl–carbonyl interactions. Coleman et al. [15] have used the frequency difference ($\Delta\nu$) between the hydrogen bonded hydroxyl absorption and free hydroxyl absorption to access the average

strength of the intermolecular interaction. Therefore, the hydroxyl–hydroxyl self-interaction is stronger than the hydroxyl–carbonyl inter-association from Figure 4.5 for POSS-PMMA/phenolic and PMMA/phenolic blends. These results are in agreement with the negative q value of PMMA obtained from the Kwei equation. However, these results are not in agreement with the positive q value of POSS-PMMA obtained from the Kwei equation. The positive q value of POSS-PMMA is because the POSS segments of the POSS-PMMA affect the interaction between PMMA and phenolic resins.

Figure 4.6 shows the infrared spectra of the carbonyl stretching measured at room temperature ranging from 1675 to 1765 cm^{-1} for different compositions of the POSS-PMMA/phenolic and PMMA/phenolic blends. For the MMA unit, the IR carbonyl stretching absorptions by free and hydrogen-bonded carbonyl groups are at 1730 and 1705 cm^{-1} , respectively [14]. It clearly shows that the fraction of hydrogen bonded carbonyl in the PMMA system is greater than that of POSS-PMMA system as shown in Figure 4.6. By quantitative measuring the absorptivity ratio of the hydrogen bonded to the free carbonyl bands in a blend system, we can determine the fraction of hydrogen bonded carbonyl of the PMMA by using the $a_R = a_{\text{HB}}/a_{\text{F}} = 1.5$ [16, 17]. Through least-squares curve-fitting within the carbonyl stretching region using two Gaussian bands. The parameters of the infrared carbonyl band are summarized in Table 4.1, where the hydrogen bonded carbonyl fraction of POSS-PMMA or PMMA increases with the increase of the phenolic content. Figure 4.7 plots the fraction of hydrogen bonded carbonyl from POSS-PMMA or PMMA vs. the phenolic weight fraction of these two blend systems. It is shown that the inter-association equilibrium constant of the PMMA/phenolic blends is LPMMA/phenolic blends > HPMMA/phenolic blends \sim POSS-HPMMA/phenolic blends > POSS-LPMMA/phenolic blends. The POSS segments of the POSS-PMMA changes the interaction between phenolic and PMMA, especially at lower molecular weight of PMMA.

4.3.4 2D IR Analyses

Figures 4.8 (a), 4.8 (b) and 4.8 (c) show the synchronous 2D IR correlation maps of PMMA/phenolic blends and POSS-PMMA/phenolic blends in the range of 1200 to 1800 cm^{-1} . The molecular weight of PMMA in Figure 4.8 is about 10,000 g mol^{-1} . Bands in Figure 4.8 (a) are mainly 1750 cm^{-1} for the carboxyl group of PMMA and 1510 cm^{-1} for the phenyl group of phenolic resins. Two strong auto and cross peaks between 1510 and 1750 cm^{-1} indicate the specific interactions. Figure 4.8 (c) shows the effect of POSS fragment. The intensity of auto and cross peaks of 1510 cm^{-1} for the phenyl group of phenolic resins becomes weakly after POSS incorporating into chain end of PMMA. Results demonstrate that the bulky end group of POSS would play a physical constraint for the conformation of phenolic resins. Therefore, the flipping motions of phenyl rings on phenolic resins have a larger external perturbation angular frequency ($\sim 180^\circ$). The reduced cross-correlation function ($X(\tau)$) produced by Noda [18].

$$X(\tau) = \Phi(v_1, v_2) \times \cos(\omega\tau) + \Psi(v_1, v_2) \times \sin(\omega\tau) \quad (2)$$

In Eq. (2), the terms, $\Phi(v_1, v_2)$ and $\Psi(v_1, v_2)$ are regarded as the real and imaginary parts of the function and are referenced as the cross peak intensities in asynchronous and synchronous correlation maps. ω is the external perturbation angular frequency, in the case of $\omega=180$, the $\cos(\omega\tau)$ equals to zero and $\sin(\omega\tau)$ equals -1.0 ; therefore, we would get the weakest cross-peak intensity in synchronous correlation maps.

Peaks corresponded to the Si-O-Si of POSS in Figure 4.8 (b) and 4.8 (c) are 1250 and 1100 cm^{-1} , both of them has a weak auto peak indicates that the amount of POSS is with a low concentration in blends. Stronger cross peaks between 1250 and 1750 cm^{-1} indicate the specific interactions contributed from siloxane bond of POSS and carboxyl of PMMA. This additional interaction also causes a decrease in the intensity of cross peaks of phenyl of phenolic resins.

The engagement molecular weight of PMMA is 18,000 g mol^{-1} . In the following case in

Figure 4.9 (a) and 4.9 (b), we demonstrate the behavior of POSS in the PMMA/phenolic blends in which the molecular weight of PMMA is about $30,000 \text{ g mol}^{-1}$. Figure 4.9 (a) has a similar pattern with Figure 4.8 (a) but with stronger cross peaks at several positions: 1750 to 1510 and 1420 cm^{-1} ; 1510 to 1200 cm^{-1} . 1200 and 1420 cm^{-1} corresponds to the methyl group and C-O of PMMA, respectively. Figure 4.9 (b) has a quite similar pattern with Figure 4.8 (b). Results show that increasing the molecular weight of PMMA increases the specific interactions in PMMA/phenolic blends. The incorporation of POSS into PMMA decreases the interaction between PMMA and phenolic resins at lower molecular weight of PMMA. As the molecular weight of PMMA is above its entanglement molecular weight, the contribution of POSS could be ignored.



4.4 Conclusions

Organic-inorganic polymer hybrids were prepared by ATRP method. POSS-PMMA/phenolic and PMMA/phenolic blends were investigated by using DSC, FT-IR, and 2D IR. All these blends are totally miscible in the amorphous phase over entire compositions. The T_g of the POSS-PMMA/phenolic blend is higher than that of the PMMA/phenolic blend. The positive q value of POSS-PMMA/phenolic blends decreases with the increase of molecular weight of POSS-PMMA. The negative q value of PMMA/phenolic blends also decreases with the increase of molecular weight of PMMA. The homogeneity of the POSS-PMMA polymer blends can be rationalized in terms of extent of hydrogen-bonding interaction, and the fraction of the hydrogen bonded carbonyl from POSS-PMMA polymer is smaller than the PMMA polymer based on FT-IR analyses. This result indicates that the POSS segments of the POSS-PMMA decreases the hydrogen bonded carbonyl interaction between PMMA and phenolic resins at lower molecular weight of PMMA, but increases inter-association interaction between polymers. As the molecular weight of PMMA is above its entanglement molecular weight, the contribution of POSS could be ignored.